

Kibble-Zurek scaling due to environment temperature quench in the transverse field Ising model

Ádám Bácsi^{1,2,*} and Balázs Dóra^{1,3}

¹*MTA-BME Lendület Topology and Correlation Research Group,
Budapest University of Technology and Economics, Műegyetem rkp. 3., H-1111 Budapest, Hungary*

²*Department of Mathematics and Computational Sciences,
Széchenyi István University, 9026 Győr, Hungary*

³*Department of Theoretical Physics, Institute of Physics,
Budapest University of Technology and Economics, Műegyetem rkp. 3., H-1111 Budapest, Hungary*

(Dated: March 9, 2022)

The Kibble-Zurek mechanism applies to defect production due to non-adiabatic passage to or through a quantum critical point (QCP). Here we study its variant from ramping the temperature to a QCP. This is achieved by studying the Lindblad equation for the transverse field Ising chain in the presence of thermalizing bath, with couplings to environment obeying detailed balance. By ramping the environment temperature with speed $1/\tau$ to the QCP, we find that the defect density scales as $\tau^{-d\nu}$ with d and ν the spatial dimensionality and the critical exponent of the correlation length, respectively. This reduced defect density, compared to conventional Kibble-Zurek mechanism, stems from the enhanced relaxation due to bath-system interaction. By temperature quenching to the gapped phases, the defect density gets exponentially suppressed with τ . The von-Neumann or the system-bath entanglement entropy follows the same scaling.

Introduction. Non-adiabatic dynamics and quantum quenches have been investigated intensively both experimentally and theoretically[1, 2]. This allows us to address fundamental questions such as thermalization and equilibration, to introduce non-equilibrium quantum fluctuation relations[3], to analyze non-linear response. The most archetypical feature is the Kibble-Zurek mechanism[4–6], which describes universal features of defect production for near adiabatic passages across quantum critical points[1, 2, 7–14]. This theory finds application in diverse fields of physics, ranging from quantum and statistical mechanics through cosmology and cold atomic systems to condensed matter physics.

The basic idea behind Kibble-Zurek theory is that when a system is driven to[12, 13] or through[6, 7] the quantum critical point (QCP) by ramping some control parameter, it undergoes an adiabatic-diabatic transition[15]. In the adiabatic phase, the system has enough time to adjust itself to the new thermodynamic conditions, therefore follows its equilibrium state and the defect production is negligible. On the other hand, upon entering into the diabatic regime, the relaxation time of the system is longer than the timescale associated to the drive. Therefore, the system cannot adjust itself to new equilibrium conditions and defects are inevitably produced. The density of defects depends on the rate of change of the control parameter and certain equilibrium critical exponents.

So far, the Kibble-Zurek mechanism has been exhaustively investigated in closed quantum systems. Recently, there is a surge of interest towards open quantum systems and non-hermitian Hamiltonians[16–20]. These focus on open quantum systems, where dissipation and decoherence through gain and loss and Lindblad dynamics

take place. In addition, the Lindblad equation opens the door to study thermalization dynamics by incorporating the principle of detailed balance in the couplings to the environment[21–25]. Various aspects of the Kibble-Zurek idea has been discussed under dissipative conditions[26–30].

We generalize the Kibble-Zurek scaling for quantum systems containing a QCP, namely the transverse field Ising chain, and coupled to a thermalizing bath within the Lindblad equation. In this case, the relaxation is dominated by the system-bath coupling and not by the intrinsic relaxation scale of the QCP. By ramping down the environment temperature to reach the QCP, we find that the defect density obeys a universal scaling, distinct from the conventional Kibble-Zurek scenario, even when the initial temperature is relatively high. This is attributed to the enhanced relaxation due to bath-system interaction. The thermodynamic entropy of the systems also follows the same scaling.

Kibble-Zurek scaling through driving the environment temperature. Let us warm up with the Kibble-Zurek scaling in closed quantum systems before generalizing it to an open one. In both cases, we use the temperature as a control parameter but it only appears in the Hamiltonian as a formal variable characterizing the strength of e.g. interaction or potential for closed quantum system while for open systems, it corresponds to the environment temperature. We assume that a quantum critical point (QCP) is located at $T = 0$, but our approach can be generalized to finite temperature phase transitions as well. When the critical point is approached, the adiabatic-diabatic transition occurs when the rate, at which we drive the system through $T(t)$, becomes comparable to the inverse of the relaxation time τ_{rel} . The relaxation

time scales with the temperature T as $\tau_{\text{rel}} \sim T^{-z\nu}$ with z and ν the dynamical critical exponent and the exponent associated to the correlation length. The adiabatic-diabatic transition occurs when these two time scales become comparable, namely

$$\frac{1}{T} \left| \frac{dT}{dt} \right| \sim T^{z\nu}. \quad (1)$$

We focus on linear cooling as $T(t) = T_0(1 - t/\tau)$ with T_0 the initial temperature and τ^{-1} measuring the rate of change. From Eq. (1), the adiabatic-diabatic transition temperature is $T(t_{tr}) \sim (1/\tau)^{1+z\nu}$ at the transition time t_{tr} . This temperature governs the scaling properties during the diabatic phase of the quench. The correlation length scales as $\xi \sim 1/(T(t_{tr}))^\nu$ and in a d -dimensional system, and the density of defects follows

$$n \sim \xi^{-d} \sim \left(\frac{1}{\tau} \right)^{\frac{\nu d}{1+z\nu}}. \quad (2)$$

However, for an open quantum system, the thermalizing environment possesses a definite temperature, which appears in the system-bath couplings. In this case, the relaxation properties of the system is dominated by the interaction with the environment rather than the internal relaxation processes, and the adiabatic-diabatic transition is determined by the bath-system coupling constant γ . Hence, the rate of change of the temperature should be compared to γ and *not* to the inherent relaxation time of the system, i.e.

$$\frac{1}{T} \left| \frac{dT}{dt} \right| \sim \gamma. \quad (3)$$

In the case of linear cooling, the adiabatic-diabatic transition happens at time $1/\gamma$ before the critical point is reached. The temperature at this time instant is $T(t_{tr}) = T_0/\gamma\tau$ and $\xi \sim 1/(T(t_{tr}))^\nu$. Then, the defect density with respect to the thermal expectation value is

$$n \sim \xi^{-d} \sim \left(\frac{T_0}{\gamma\tau} \right)^{\nu d} \quad (4)$$

This scaling behavior differs from Eq. (2) and also predicts not only the τ , but also the T_0 and γ dependence of the defect density. For a given τ , the defect density is suppressed due to the missing denominator $1 + \nu z$ in the exponent. The lower defect density is the consequence of the enhanced relaxation stemming from the bath-system interaction compared to the diverging relaxation time (and vanishing energy scale) for closed quantum systems.

Transverse field Ising chain. The paradigmatic example of a quantum phase transition is represented by the one-dimensional transverse field Ising model[6, 31–34] We demonstrate how the scaling behaviour in Eq. (4) emerges explicitly in a system whose dynamics is governed by the Lindblad equation. The model is described

by the Hamiltonian of spin- $\frac{1}{2}$ s as

$$H = -J \sum_j (g S_j^x + S_j^z S_{j+1}^z) \quad (5)$$

where j runs over the sites of the one-dimensional chain and $J > 0$. The number of sites is N and the length of the chain is $L = Na$ with a the lattice constant. The dimensionless coupling $g > 0$ measures the strength of the transverse field. With a Jordan-Wigner transformation[35], Fourier transformation to momentum space and a Bogoliubov transformation, the the Hamiltonian reduces to

$$H = E_0 + \sum_{k>0, s=\pm} E_k d_{ks}^+ d_{ks} \quad (6)$$

where $E_0 = -\sum_{k>0} E_k$ is the ground state energy and $E_k = 2J\sqrt{(g - \cos(ka))^2 + \sin^2(ka)}$ is the energy spectrum of the fermionic excitations and d_{ks} are fermionic operators. In the Hamiltonian, the sum runs over the wavenumbers $k = (2n + 1)\pi/L$ with an integer n [36].

The density of states as a function of energy is calculated as

$$G(E) = \frac{N}{\pi J} \left(2(g^2 + 1) - (g^2 - 1)^2 \left(\frac{2J}{E} \right)^2 - \left(\frac{E}{2J} \right)^2 \right)^{-\frac{1}{2}}. \quad (7)$$

The domain of $G(E)$ is $\Delta < E < 2J|g + 1|$ with $\Delta = 2J|g - 1|$ being the gap.

For $g = 1$, the spectrum is gapless and the system realizes a QCP with critical exponents $z = \nu = 1$ [31] and $d = 1$. The QCP separates ferromagnetic ($g < 1$) and paramagnetic ($g > 1$) phases. In Ref. [6], the quantum quench between the two phases has been studied, i.e., when the system is driven along the g axis through the critical point at $g = 1$ and zero temperature $T = 0$. In the present paper, we consider approaching the QCP from another direction on the phase diagram as illustrated in Fig. 1.

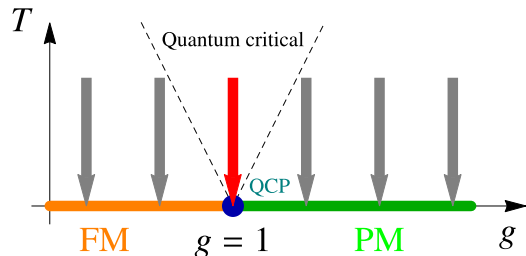


FIG. 1. Illustration of the phase diagram and the linear cooling protocol (vertical arrows) for the transverse field Ising chain at fixed transverse field. The QCP at $g = 1$ separates ferro- and paramagnetic phases.

Temperature quench to $T = 0$ within the Lindblad equation. We now couple the transverse field Ising chain to a thermalizing bath via the Lindblad equation [17, 19, 22, 37] and consider a quench in which the transverse field is kept constant while the *environment* temperature is driven linearly from a finite value to zero, see Fig. 1. This yields

$$\begin{aligned} \partial_t \rho = & -i[H, \rho] + \\ & + \sum_{ks} \gamma_{k,\uparrow} \mathcal{D}\left(L_{ks,\uparrow}; \rho; L_{ks,\uparrow}^+\right) + \gamma_{k,\downarrow} \mathcal{D}\left(L_{ks,\downarrow}; \rho; L_{ks,\downarrow}^+\right) \end{aligned} \quad (8)$$

where $\mathcal{D}(L; \rho; L^+) = L\rho L^+ - \{L^+L, \rho\}/2$. In order to thermalize the system, two jump operators are considered for each k and s , which couple to the eigenstates of the Hamiltonian as $L_{ks,\uparrow} = d_{ks}^+$ and $L_{ks,\downarrow} = d_{ks}$, creating and annihilating a fermionic excitation of with quantum numbers s and k , respectively. Thermalization is ensured by requiring the couplings to environment to obey detailed balance corresponding to a bath temperature T as $\gamma_{k,\downarrow}/\gamma_{k,\uparrow} = e^{\beta E_k}$ with $\beta = 1/T$ [23].

Since the goal is to investigate a time-dependent variation of temperature, the temperature dependence of the coupling constants $\gamma_{k,\downarrow}$ and $\gamma_{k,\uparrow}$ is essential. The condition of detailed balance determines their ratio only, while an explicit temperature dependence would follow by performing microscopic derivation of bath correlation functions [23, 38]. For a system of the type in Eq. (8), the temperature dependence is determined by [25, 38]

$$\gamma_{k,\downarrow} = \gamma \frac{1}{1 + e^{-\beta E_k}} \quad \text{and} \quad \gamma_{k,\uparrow} = \gamma \frac{1}{1 + e^{\beta E_k}}. \quad (9)$$

The transition rate γ is already independent from temperature. We note that the Lindbladian Eq. (8) is one of many possible choices to describe detailed balance, more involved jump processes between states of different wavenumbers could also be included. However, for the sake of simplicity and physical relevance, we focus on the most obvious dissipative processes.

In the followings, we assume that the temperature decreases from an initial temperature T_0 to zero as

$$T(t) = T_0 \left(1 - \frac{t}{\tau}\right), \quad 0 < t < \tau, \quad (10)$$

and describes linear cooling. Consequently, through $\beta(t) = 1/T(t)$, the coupling constants $\gamma_{ks,\uparrow}$ and $\gamma_{ks,\downarrow}$ depend on time.

Assuming thermal equilibrium at $t = 0$, the probability that the state ks is filled with a fermion is calculated from the Lindblad equation as [35]

$$\langle d_{ks}^+ d_{ks} \rangle \equiv p_k(t) = \frac{e^{-\gamma t}}{1 + e^{\beta_0 E_k}} + \gamma \int_0^t \frac{e^{-\gamma(t-t')}}{1 + e^{\beta(t') E_k}} dt'. \quad (11)$$

Defect density. The total density of defects is obtained as

$$n(t) = \frac{1}{N} \sum_{ks} p_k(t), \quad (12)$$

which represents kinks in the FM state [6, 31] or the transverse magnetization in the PM phase. For a perfectly adiabatic quench, the system would reach its ground state and no defects would be present. For finite quench duration, however, a finite number of defects is generated at the end of the quench due to the adiabatic-diabatic transition.

The final density of defects $n(\tau)$ depends strongly on whether the system is critical or gapped, which influences the behaviour of the density of states in Eq. (7) at low energies. For the critical gapless system ($g = 1$), the density of states is constant, $G(E) \sim \text{const.}$ down to $E = 0$, while in the gapped phase ($|g - 1| \gg 0$), the density of state diverges as $G(E) \sim \sqrt{E/(E - \Delta)}$ at the gap edge, $E \gtrsim \Delta$.

In principle, for the gapped phase, the number of defects after the temperature ramp is expected to be exponentially suppressed on general ground, while at or very close to the QCP, a power-law dependence as in Eq. (4) is expected.

We start with the behaviour in the gapped phases. The final density of defects is obtained as [35]

$$\begin{aligned} n(\tau) = & \frac{1}{8} \sqrt{\frac{|1-g|}{\beta_0 J g}} \sum_{j=\pm 1} e^{2j\sqrt{\beta_0 \Delta} \gamma \tau} \left(2\sqrt{\beta_0 \Delta} - \frac{j}{\sqrt{\gamma \tau}} \right) \times \\ & \times \left[1 - \Phi\left(\sqrt{\beta_0 \Delta} + j\sqrt{\gamma \tau}\right) \right] \end{aligned} \quad (13)$$

for the cases when g is far from 1 with $\Phi(x)$ the error function [39]. For near-adiabatic quenches in the gapped case (g far from 1) with both $1 \ll \beta_0 \Delta$ and $1 \ll \gamma \tau$, we find that

$$n(\tau) = \frac{|1-g|}{\sqrt{2g}} \times \begin{cases} e^{-2\sqrt{\beta_0 \Delta} \gamma \tau}, & \beta_0 \Delta \ll \gamma \tau \\ \frac{e^{-\beta_0 \Delta - \gamma \tau}}{\sqrt{\pi \beta_0 \Delta}}, & \beta_0 \Delta \gg \gamma \tau \end{cases}. \quad (14)$$

In both cases, the number of defects vanishes exponentially with $\gamma \tau$ for long quenches, in accord with expectations.

For the gapless case, $g = 1$, the final density of defects follows a power-law dependence as

$$n(\tau) = \frac{\ln 2}{2\pi \beta_0 J} \frac{1 - e^{-\gamma \tau}}{\gamma \tau} \xrightarrow{\gamma \tau \rightarrow \infty} \frac{T_0 \ln 2}{2\pi J} \frac{1}{\gamma \tau}. \quad (15)$$

We have also studied the full lattice version of the model by performing the energy and the temporal integrals numerically in Eqs. (11) and (12). Eqs. (13)-(15) agree nicely with the numerically exact results in Fig. 2 including the $\gamma \tau$ and T_0 dependences. Eq. (15) indeed shows the expected power-law decay in the adiabatic

limit, $\tau \gg \gamma^{-1}$ as $\tau^{-\nu d}$ with $\nu = d = 1$. The exponent of the decay differs from the conventional Kibble-Zurek exponent from Eq. (2), which would predict $n(\tau) \sim \tau^{-1/2}$ for the transverse field Ising model [6]. The difference can be explained by the bath-system interaction preventing the system from "critical slowing down" and enhancing relaxation throughout the diabatic phase.

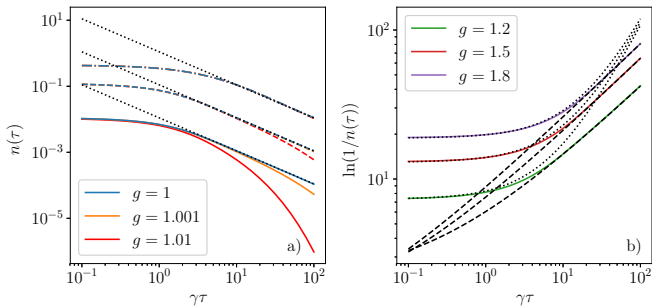


FIG. 2. Numerical results for the density of defects, $n(\tau)$, at the end of the quench for various values of g . a) Cooling to or very close to the QCP. The solid, dashed and dash-dotted line corresponds to the initial temperature of $T_0/J = 0.1, 1$ and 10 , respectively. For each initial temperature, the black dotted line shows the τ^{-1} behavior of Eq. (15). b) Far from the QCP, the numerical results (solid lines) agree with Eq. (14) (dashed and dotted lines) in limiting cases, the initial temperature is $T_0/J = 0.1$.

Entropy. While closed quantum systems are typically described by a wavefunction, open quantum systems possess a density matrix. This allows us to calculate the thermodynamic entropy after the temperature ramp, which also quantifies the entanglement between the system of interest and its environment. The entropy change represents a useful measure of the adiabaticity of the quench. For the transverse field Ising model, after a perfectly adiabatic quench, the system is expected to reach the pure ground state with vanishing entropy. For a quench of finite duration, however, some entropy is unavoidably generated. The irreversible entropy production from Kibble-Zurek theory was touched upon in Ref. [40]. Based on the occupation probabilities $p_{ks}(t)$ in Eq. (11), the entropy is

$$S(t) = - \sum_{ks} (p_k(t) \ln p_k(t) + (1 - p_k(t)) \ln(1 - p_k(t))). \quad (16)$$

The final entropy, $S(\tau)$, depends on the final occupation probabilities $p_k(\tau)$.

In the gapped phase with $1 \ll \beta_0 \Delta \ll \gamma \tau$, the final entropy is obtained as $S(\tau) \approx 2Nn(\tau)$, displayed in Fig. 3. Similarly to the defect density, the most interesting case involves quench to the gapless, critical system with $g = 1$. For long quenches, $\gamma \tau \gg 1$, the final occupation

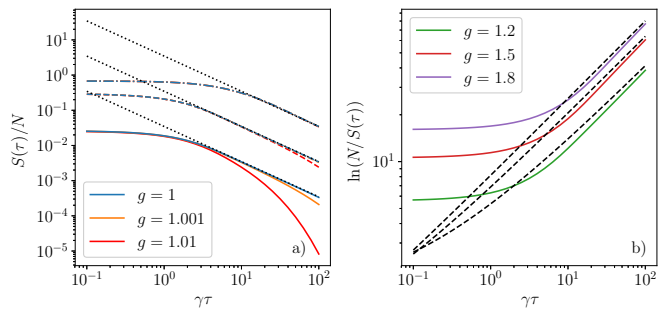


FIG. 3. Numerical results for the entropy, $S(\tau)$, at the end of the quench for various values of g . a) Cooling to or very close to the QCP. The solid, dashed and dash-dotted line corresponds to the initial temperature of $T_0/J = 0.1, 1$ and 10 , respectively. For each initial temperature, the black dotted line shows the τ^{-1} behavior of Eq. (18). b) Numerical results far from the QCP with the initial temperature $T_0/J = 0.1$, the black dashed lines denote $2Nn(\tau)$.

probabilities $p_k(\tau)$ are approximated as

$$p_k(\tau) = \int_0^\infty \frac{e^{-y}}{1 + e^{\frac{\beta_0 E_k \gamma \tau}{y}}} dy \quad (17)$$

which depend only on $\beta_0 E_k \gamma \tau$ only. Substituting this into Eq. (16) and using $\sum_{ks} \rightarrow \int dE G(E)$ in the thermodynamic limit, we get

$$S(\tau) \approx \frac{NT_0 \ln 2}{2J\gamma\tau}. \quad (18)$$

The final entropy is plotted in Fig. 3 and is in good agreement with the numerical result for long quenches. For quenches terminating away from the QCP, the entropy gets exponentially suppressed in τ , similarly to the defect density. This indicates that the entropy follows also a universal Kibble-Zurek scaling.

Conclusion. We have studied the effect of cooling the environment temperature to a QCP, and its influence on Kibble-Zurek scaling. We find that the diverging relaxation time, associated to QCP, gets replaced by the inverse coupling to environment, which results in a modified, but universal scaling of the defect density. By investigating the dissipative version of the transverse field Ising chain, we verify this prediction and also find that by ramping down the temperature to a gapped ground state, the defect density follows an exponential scaling with the ramp time. The system-bath entanglement entropy follows the same universal scaling and should be accessible experimentally, together with the defect density[8].

We thank B. Gulácsi for useful discussions. This research is supported by the National Research, Development and Innovation Office - NKFIH within the Quantum Technology National Excellence Program (Project No. 2017-1.2.1-NKP-2017-00001), K134437, by the BME-Nanotechnology FIKP grant (BME FIKP-NAT), and by

a grant of the Ministry of Research, Innovation and Digitization, CNCS/CCCDI-UEFISCDI, under projects number PN-III-P4-ID-PCE-2020-0277.

* bacsi.adam@sze.hu

- [1] A. Polkovnikov, K. Sengupta, A. Silva, and M. Vengalattore, *Colloquium : Nonequilibrium dynamics of closed interacting quantum systems*, Rev. Mod. Phys. **83**, 863 (2011).
- [2] J. Dziarmaga, *Dynamics of a quantum phase transition and relaxation to a steady state*, Adv. Phys. **59**, 1063 (2010).
- [3] M. Campisi, P. Hänggi, and P. Talkner, *Colloquium : Quantum fluctuation relations: Foundations and applications*, Rev. Mod. Phys. **83**, 771 (2011).
- [4] T. W. B. Kibble, *Topology of cosmic domains and strings*, J. Phys. A **9**, 1387 (1976).
- [5] W. H. Zurek, *Cosmological experiments in superfluid helium?*, Nature **317**, 505 (1985).
- [6] J. Dziarmaga, *Dynamics of a quantum phase transition: Exact solution of the quantum ising model*, Phys. Rev. Lett. **95**, 245701 (2005).
- [7] A. Polkovnikov, *Universal adiabatic dynamics in the vicinity of a quantum critical point*, Phys. Rev. B **72**, 161201 (2005).
- [8] A. Keesling, A. Omran, H. Levine, H. Bernien, H. Pichler, S. Choi, R. Samajdar, S. Schwartz, P. Silvi, S. Sachdev, P. Zoller, M. Endres, et al., *Quantum kibble-zurek mechanism and critical dynamics on a programmable rydberg simulator*, Nature **568**, 207 (2019).
- [9] J. Beugnon and N. Navon, *Exploring the kibble-zurek mechanism with homogeneous bose gases*, Journal of Physics B: Atomic, Molecular and Optical Physics **50**(2), 022002 (2017).
- [10] B. Ko, J. W. Park, and Y. Shin, *Kibble-zurek universality in a strongly interacting fermi superfluid*, Nat. Phys. **15**, 1227 (2019).
- [11] L. Xiao, D. Qu, K. Wang, H.-W. Li, J.-Y. Dai, B. Dóra, M. Heyl, R. Moessner, W. Yi, and P. Xue, *Non-hermitian kibble-zurek mechanism with tunable complexity in single-photon interferometry*, PRX Quantum **2**, 020313 (2021).
- [12] B. Damski and W. H. Zurek, *How to fix a broken symmetry: quantum dynamics of symmetry restoration in a ferromagnetic bose-einstein condensate*, New Journal of Physics **10**(4), 045023 (2008).
- [13] M. Białończyk and B. Damski, *One-half of the kibble-zurek quench followed by free evolution*, Journal of Statistical Mechanics: Theory and Experiment **2018**(7), 073105 (2018).
- [14] L.-Y. Qiu, H.-Y. Liang, Y.-B. Yang, H.-X. Yang, T. Tian, Y. Xu, and L.-M. Duan, *Observation of generalized kibble-zurek mechanism across a first-order quantum phase transition in a spinor condensate*, Science Advances **6**(21), eaba7292 (2020).
- [15] A. del Campo, A. Retzker, and M. B. Plenio, *The inhomogeneous kibble-zurek mechanism: vortex nucleation during bose-einstein condensation*, New Journal of Physics **13**(8), 083022 (2011).
- [16] R. El-Ganainy, K. G. Makris, M. Khajavikhan, Z. H. Musslimani, S. Rotter, and D. N. Christodoulides, *Non-hermitian physics and pt symmetry*, Nat. Phys. **14**(1), 11 (2018).
- [17] I. Rotter and J. P. Bird, *A review of progress in the physics of open quantum systems: theory and experiment*, Rep. Prog. Phys. **78**, 114001 (2015).
- [18] C. M. Bender and S. Boettcher, *Real spectra in non-hermitian hamiltonians having PT symmetry*, Phys. Rev. Lett. **80**, 5243 (1998).
- [19] Y. Ashida, Z. Gong, and M. Ueda, *Non-hermitian physics*, Advances in Physics **69**, 3 (2020).
- [20] E. J. Bergholtz, J. C. Budich, and F. K. Kunst, *Exceptional topology of non-hermitian systems*, Rev. Mod. Phys. **93**, 015005 (2021).
- [21] A. Rajagopal, *The principle of detailed balance and the lindblad dissipative quantum dynamics*, Physics Letters A **246**(3), 237 (1998).
- [22] H. Carmichael, *An Open Systems Approach to Quantum Optics* (Springer-Verlag, Berlin, 1993).
- [23] H. Breuer and F. Petruccione, *The Theory of Open Quantum Systems* (Oxford University Press, 2002).
- [24] M. Palmero, X. Xu, C. Guo, and D. Poletti, *Thermalization with detailed-balanced two-site lindblad dissipators*, Phys. Rev. E **100**, 022111 (2019).
- [25] I. Reichental, A. Klemmner, Y. Kafri, and D. Podolsky, *Thermalization in open quantum systems*, Phys. Rev. B **97**, 134301 (2018).
- [26] D. Rossini and E. Vicari, *Dynamic kibble-zurek scaling framework for open dissipative many-body systems crossing quantum transitions*, Phys. Rev. Research **2**, 023211 (2020).
- [27] W.-T. Kuo, D. Arovass, S. Vishveshwara, , and Y.-Z. You, *Decoherent quench dynamics across quantum phase transitions*, SciPost Phys. **11**, 84 (2021).
- [28] M. Keck, S. Montangero, G. E. Santoro, R. Fazio, and D. Rossini, *Dissipation in adiabatic quantum computers: lessons from an exactly solvable model*, New Journal of Physics **19**(11), 113029 (2017).
- [29] A. Zamora, G. Dagvadorj, P. Comaron, I. Carusotto, N. P. Proukakis, and M. H. Szymańska, *Kibble-zurek mechanism in driven dissipative systems crossing a nonequilibrium phase transition*, Phys. Rev. Lett. **125**, 095301 (2020).
- [30] P. Hedvall and J. Larson, *Dynamics of non-equilibrium steady state quantum phase transitions*, arXiv:1712.01560.
- [31] S. Sachdev, *Quantum Phase Transitions* (Cambridge Univ. Press, Cambridge, 1999).
- [32] A. Dutta, G. Aeppli, B. K. Chakrabarti, U. Divakaran, T. F. Rosenbaum, and D. Sen, *Quantum Phase Transitions in Transverse Field Spin Models: From Statistical Physics to Quantum Information* (Cambridge University Press, 2015).
- [33] R. Coldea, D. A. Tennant, E. M. Wheeler, E. Wawrzynska, D. Prabhakaran, M. Telling, K. Habicht, P. Smeibidl, and K. Kiefer, *Quantum criticality in an ising chain: Experimental evidence for emergent es symmetry*, Science **327**, 177 (2010).
- [34] A. W. Kinross, M. Fu, T. J. Munsie, H. A. Dabkowska, G. M. Luke, S. Sachdev, and T. Imai, *Evolution of quantum fluctuations near the quantum critical point of the transverse field ising chain system conb₂o₆*, Phys. Rev. X **4**, 031008 (2014).
- [35] See EPAPS Document No. XXX for supplementary material providing further technical details.

- [36] This quantization corresponds to an antiperiodic boundary condition for the fermionic c operators which is in accordance with periodic boundary condition for the spins [6].
- [37] A. J. Daley, *Quantum trajectories and open many-body quantum systems*, *Advances in Physics* **63**, 77 (2014).
- [38] A. D'Abbruzzo and D. Rossini, *Self-consistent microscopic derivation of markovian master equations for open quadratic quantum systems*, *Phys. Rev. A* **103**, 052209 (2021).
- [39] I. Gradshteyn and I. Ryzhik, *Table of Integrals, Series, and Products* (Academic Press, New York, 2007).
- [40] S. Deffner, *Kibble-zurek scaling of the irreversible entropy production*, *Phys. Rev. E* **96**, 052125 (2017).

Diagonalization of the Hamiltonian in the transverse field Ising model

With the Jordan-Wigner transformation $S_j^z = (c_j + c_j^\dagger) \prod_{m < j} e^{i\pi \hat{n}_m}$ and $S_j^x = 1 - 2\hat{n}_j$ with $\hat{n}_j = c_j^\dagger c_j$ as introduced in Ref. [6], the Hamiltonian reads

$$H = -J \sum_j [g(1 - 2c_j^\dagger c_j) + (c_j^\dagger c_{j+1} + c_j^\dagger c_{j+1}^\dagger + h.c.)] \quad (19)$$

By applying Fourier transform to momentum space, we obtain

$$H = -NJg + 2J \sum_k \left[A_k c_k^\dagger c_k + \left(\frac{iB_k}{2} c_{-k} c_k + h.c. \right) \right] \quad (20)$$

where $A_k = g - \cos(ka)$ and $B_k = \sin(ka)$.

The Hamiltonian is diagonalized by the Bogoliubov transformation

$$\begin{aligned} c_k &= u_k d_{k+} + v_k^* d_{k-}^+ \\ c_{-k} &= u_k d_{k-} - v_k^* d_{k+}^+ \end{aligned} \quad (21)$$

where $u_k = \frac{\sqrt{1 + (1 + B_k/A_k)^{-1/2}}}{\sqrt{2}}$ and $v_k = -i \frac{\sqrt{1 - (1 + B_k/A_k)^{-1/2}}}{\sqrt{2}}$. After Bogoliubov transformation the Hamiltonian reads

$$H = E_0 + \sum_{k>0, s=\pm} E_k d_{ks}^+ d_{ks} \quad (22)$$

where $E_0 = -\sum_{k>0} E_k$ is the ground state energy and

$$E_k = 2J \sqrt{(g - \cos(ka))^2 + \sin^2(ka)} \quad (23)$$

is the energy spectrum of the fermionic excitations.

Derivation of the number of defects after temperature quench in the transverse field Ising model

In this section, the derivation of the density of defects is presented. The number of defects is defined as $\mathcal{N}_S(t) = \sum_{ks} p_k(t)$ where $p_k(t) = \langle d_{ks}^+ d_{ks} \rangle(t)$ is the occupation probability of the fermionic state corresponding to the quantum numbers k and s .

In order to determine the dynamics of $p_k(t)$, let us recall the Lindblad equation

$$\begin{aligned} \partial_t \rho &= -i [H, \rho] + \\ &+ \sum_{ks} \gamma_{k,\uparrow}(t) \mathcal{D} \left(L_{ks,\uparrow}; \rho; L_{ks,\uparrow}^+ \right) + \gamma_{k,\downarrow}(t) \mathcal{D} \left(L_{ks,\downarrow}; \rho; L_{ks,\downarrow}^+ \right) \end{aligned} \quad (24)$$

where $L_{ks,\uparrow} = d_{ks}^+$, $L_{ks,\downarrow} = d_{ks}$, $H = E_0 + \sum_{k>0,s} E_k d_{ks}^+ d_{ks}$ and the coupling constants are given by

$$\gamma_{k,\uparrow}(t) = \gamma \frac{1}{1 + e^{\beta(t)E_k}} \quad (25)$$

and $\gamma_{k,\downarrow}(t) = \gamma - \gamma_{k,\uparrow}$ with the time-dependent temperature $T(t) = T_0(1 - t/\tau)$. Note that both the unitary and the dissipative terms are diagonal in k and s . Hence, for each ks , the dynamics is restricted to a two-dimensional Hilbert space spanned by the states that ks is empty or occupied. The density matrix can, therefore, be represented by

$$\rho(t) = \prod_{k>0,s} \begin{bmatrix} 1 - p_k(t) & q_k(t) \\ q_k(t)^* & p_k(t) \end{bmatrix} \quad (26)$$

with the real-valued functions $p_k(t) = \langle d_{ks}^+ d_{ks} \rangle$ and complex-valued functions $q_k(t)$. Based on the Lindblad equation, the following equations are derived.

$$\dot{p}_k = \gamma_{k,\uparrow}(t)(1 - p_k(t)) - \gamma_{k,\downarrow}(t)p_k(t) \quad (27a)$$

$$\dot{q}_k = \left(i\Delta - \frac{\gamma_{k,\uparrow}(t) + \gamma_{k,\downarrow}(t)}{2} \right) q_k(t) \quad (27b)$$

If $\gamma_{k,\uparrow}$ and $\gamma_{k,\downarrow}$ did not change with time, the steady state of Eq. (27) would be $q_{k,\infty} = 0$ and $p_{k,\infty} = (1 + \gamma_{k,\downarrow}/\gamma_{k,\uparrow})^{-1} = (1 + e^{\beta E_k})^{-1}$ describing thermal equilibrium.

In our model, we assume that the initial condition is the thermal equilibrium state corresponding to the initial temperature T_0 , i.e., $p(0) = (1 + e^{\beta_0 E})^{-1}$ with $\beta_0 = T_0^{-1}$ and $q(0) = 0$. The inhomogeneous differential equations in Eqs. (27) are solved by

$$p_k(t) = \frac{e^{-\gamma t}}{1 + e^{\beta_0 E_k}} + \gamma \int_0^t \frac{e^{-\gamma(t-t')}}{1 + e^{\beta(t')E_k}} dt' \quad (28)$$

and $q_k(t) = 0$ for the time interval $0 < t < \tau$. After the temperature quench, i.e., when the cooling has already ended and the temperature is constant zero, we obtain $p(t > \tau) = p(\tau)e^{-\gamma(t-\tau)}$.

The time dependence of $p(t)$ is evaluated numerically and is shown in Fig. 4 for several quench durations. In the figure, dashed lines show the probability for the system in thermal equilibrium at the instantaneous temperature. It can be observed that for long quenches, the time evolution follows closely the equilibrium values but for short quenches, they differ significantly.

The final number of defects is obtained by summing up Eq. (28) leading to

$$\mathcal{N}_S(t) = F(\beta_0)e^{-\gamma t} + \gamma \int_0^t e^{-\gamma(t-t')} F(\beta(t')) dt' \quad (29)$$

where

$$F(\beta) = \int_{\Delta}^{2J|g+1|} dE \frac{G(E)}{1 + e^{\beta E}} \quad (30)$$

is the expectation value of the total number of fermionic excitations in the system where $\Delta = 2J|g-1|$ is the gap.

We are mostly interested in the low-temperature behavior, i.e., when the temperature is much lower than the bandwidth during the whole quench, $T_0 \ll 2J$. In this situation, only low-energy states are occupied for which the density of states is approximated as

$$G(E) \approx \frac{N}{2\pi J} \begin{cases} \sqrt{\frac{E}{2g(E-\Delta)}} & \text{if } g \text{ is far from } 1 \\ 1 & \text{if } g = 1 \end{cases} \quad (31)$$

and the function $F(\beta)$ is computed as

$$\frac{F(\beta)}{N} \approx \begin{cases} \sqrt{\frac{|g-1|}{4\pi g\beta J}} e^{-\beta\Delta} & \text{if } g \text{ is far from } 1 \\ \frac{\ln 2}{2\pi\beta J} & \text{if } g = 1 \end{cases} \quad (32)$$

where the upper limit of the integral in Eq. (30) has been set to infinity.

Numerical investigations show that the approximate functions in Eq. (32) are in good agreement with the numerically evaluated Eq. (30) at low temperatures.

Substituting Eqs. (32) into Eq. (29), we obtain

$$\begin{aligned} n(t) &= \frac{\mathcal{N}_S(t)}{N} = \sqrt{\frac{|1-g|}{4\pi J\beta_0 g}} \left(1 - \frac{t}{\tau}\right) e^{-\frac{\beta_0 \Delta}{1 - \frac{t}{\tau}}} + e^{-\gamma t} \sqrt{\frac{|1-g|}{64J\beta_0 g}} e^{-\beta_0 \Delta} \sum_{j=\pm 1} e^{(\sqrt{\beta_0 \Delta} + j\sqrt{\gamma\tau})^2} \times \\ &\times \left(2\sqrt{\beta_0 \Delta} - \frac{j}{\sqrt{\gamma\tau}}\right) \left[\Phi\left(\frac{\sqrt{\beta_0 \Delta}}{\sqrt{1 - \frac{t}{\tau}}} + j\sqrt{\gamma\tau}\sqrt{1 - \frac{t}{\tau}}\right) - \Phi\left(\sqrt{\beta_0 \Delta} + j\sqrt{\gamma\tau}\right) \right] \end{aligned} \quad (33)$$

if g is far from 1 and

$$n(t) = \frac{\ln 2}{2\pi J\beta_0} \left(1 - \frac{t}{\tau} + \frac{1 - e^{-\gamma t}}{\gamma\tau}\right) \quad (34)$$

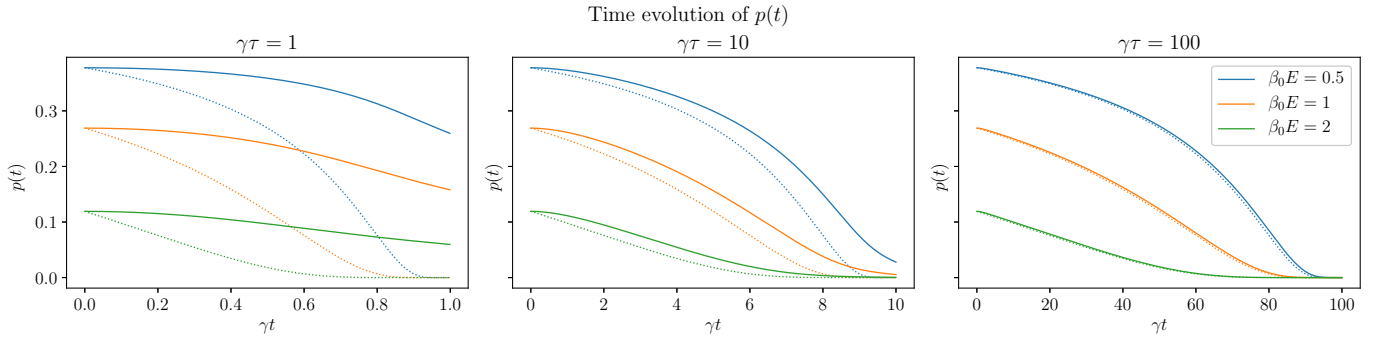


FIG. 4. The time evolution of occupation probability for different quench duration. The solid line is the numerical solution of Eq. (28) while the dashed line corresponds to the system in thermal equilibrium at the instantaneous temperature.

if $g = 1$. At the end of the quench, $t = \tau$, the density of defects is calculated as

$$n(\tau) = \sqrt{\frac{|1-g|}{64J\beta_0g}} \sum_{j=\pm 1} e^{2j\sqrt{\beta_0\Delta}\gamma\tau} \left(2\sqrt{\beta_0\Delta} - \frac{j}{\sqrt{\gamma\tau}} \right) \left[1 - \Phi \left(\sqrt{\beta_0\Delta} + j\sqrt{\gamma\tau} \right) \right] \quad (35)$$

for g being far from 1 and

$$n(\tau) = \frac{\ln 2}{2\pi J\beta_0} \frac{1 - e^{-\gamma\tau}}{\gamma\tau} \quad (36)$$

for $g = 1$. In the formulae, $\Phi(x)$ is the error function defined as $\Phi(x) = \frac{2}{\sqrt{\pi}} \int_0^x e^{-y^2} dy$.